MILLIMETER-WAVE PROPAGATION MODELING FOR 5G BASED ON RAIN FADE DATA IN TROPICAL CLIMATE

BY

ASMA ALI HUSSEIN BUDALAL

A thesis submitted in fulfillment of the requirement for the degree of Doctor of Philosophy (Engineering)

Kulliyyah of Engineering
International Islamic University Malaysia

MARCH 2022

ABSTRACT

The demand for radio frequency spectrum is rapidly increasing to serve a large number of customers in business, government, and private sectors. Hence, 5G is forcibly moving forward to utilizing millimeter-waves frequency bands. Rain is the main source of impairments for the radio wave when the frequency is higher than 10 GHz. Rain attenuation can be obtained directly from measurement or predicted from a knowledge of rain intensity. The accuracy of rain attenuation prediction on short-range mm-waves terrestrial links is vital for signal strength prediction and link budget design for 5G systems and beyond. However, recent measurements at mm-wave with short path lengths (less than 1 km) show that all prediction models, including ITU-R P.530-17, cannot predict the measured rain attenuations. Two modifications are proposed on ITU-R P.530-17 rain attenuation model. Firstly, the distance factor is analyzed thoroughly. A modification on distance factor is presented as "Increment Factor" ($I_{f\gamma}$) for path lengths less than 1 Km and updated based on measurements at 26 and 38 GHz at 0.3km path length for one year period in Malaysia, at 25 GHz for 223 m path length in Japan and 75 GHz for 100 m path length in Korea. Secondly, an effective rain rate concept (R_{eff}) is also proposed and modeled to eliminate the need for effective path lengths, representing rain intensities variations over a very short path. Several available measurements from various geographical locations in Malaysia and abroad with different frequencies and less than 1 km path lengths were utilized to validate both models and find good agreement. Rain attenuation impacts path loss, path loss exponent, and shadow fading are analyzed using two large-scale fading path loss models namely 3GPP and NYUSIM. The randomness behaviour of rain attenuation increases path loss exponent (PLE=2.79 at $R_{0.01\%}$ =125 mm/h). The NYUSIM channel model provided a better estimation of the measured data of path loss compared with 3GPP. The close-in (CI) path loss model which has been implemented by NYUSIM is modified by including the Path Loss Exponent and Shadow Fading as a function of the percentage of availability (%P of time). The proposed probabilistic path loss model, which is a combination of the close-in reference LOS free space path loss, rain attenuation based on modified ITU-R P.530-17 and shadowing at different probabilities, can predict the path loss more accurately in tropical regions. The average path loss value is found at 132.36 dB at 38 GHz with a path length of 300 m for one year period and is located at 144.5 dB with considering shadowing in the urban region with σSF = 5.22 dB. This has been realized from the analysis that the 99.99% reliability with 300m link can be designed at 38GHz with an additional 12 dB fade margin in the tropical region. All of these findings will be beneficial to develop 5G channel models in an outdoor environment, especially for mm-wave and short-path lengths applications with high reliability.

.

خلاصة البحث

يتزايد الطلب على طيف الترددات الراديوية بسرعة لتلبيه الخدمات الجيدة لعدد كبير من العملاء في القطاعين، الحكومي والخاص. لذلك أصبح التطوير المنسق والتشغيل الفعال لأنظمة الاتصالات الراديوية القائمة والجديدة مهماً للغاية. إن أنظمة الجيل الخامس 5G وما بعدها تتحرك بقوة إلى الأمام لاستخدام نطاقات تردد الموجات المليمترية. اثبتت الدراسات ان المطر هو أحد المصادر الرئيسية لضعف الموجات اللاسلكية عندما يكون التردد أعلى من 10 جيجا هرتز. يمكن الحصول على التوهين الناجم عن المطر مباشرة من القياس أو التنبؤ به باستخدام نماذج مختلفة عند معرفة معدل كثافة المطر. تُظهر القياسات الحديثة على نطاقات تردد الموجات المليمترية مع أطوال مسارات اتصالات قصيرة المدي (أقل من كيلومتر واحد) أن جميع نماذج التنبؤ، بما في ذلك الاتحاد الدولي للاتصالات (ITU) التوصية ITU-R P.530-17 غير قادرة على التنبؤ بتوهين المطر المقاس، في حين أن دقة التنبؤ بالتوهين الناجم عن المطر على الوصلات الأرضية ذات الموجات المليمترية قصيرة المدي ذات أهمية قصوى للتنبؤ بقوة الإشارة لتقييم الأداء وتصميم ميزانية الارتباط لأنظمة الجيل الخامس وما بعدها. ومن هذا المنطلق نظراً لندره النماذج الموثوقة وطرائق التنبؤ المطلوبة التي تحسب توهين الإشارات بسبب الانتشار اثناء المطر المقاس لتصميم أنظمة راديوية في خط البصر ذات الموجات المليمترية قصيرة المدي، اقترحت هذه الدراسة تعديلين على نموذج التوهين الناجم عن المطر ITU-R P.530-17. أولاً، يتم تحليل عامل المسافة بدقة، ويُقترح تعديل عامل المسافة على أنه "عامل زيادة في التوهين المحدد" ($I_{f\gamma}$) لأطوال المسير التي تقل عن كيلومتر واحد حيث تم تحديثه وحسابه بناءً على القياسات وبيانات حقيقيه لمده سنه كامله للتوهين الناجم عن المطر عند ترددات 26 و38 جيجا هرتز عند طول المسار 0.3 كم في ماليزيا وعند 25 جيجا هرتز لطول مسار 223 مترًا في اليابان و75 جيجا هرتز لطول 100 متر في كوريا. ثانيًا، يُقترح أيضًا مفهوم معدل المطر الفعال (R_{eff}) ونمذجته لإزالة الحاجة إلى أطوال مسير فعالة، والتي يمكن أن تمثل اختلافات في شدة المطر على مسار قصير جدًا. يتم استخدام العديد من القياسات المتاحة من مواقع جغرافية مختلفة في ماليزيا وخارجها بترددات مختلفة وأطوال مسار أقل من كيلومتر واحد للتحقق من صحة كلا النموذجين والتوصل إلى اتفاق جيد والتحقق من فاعليه أداء النموذج المعدل المقترح. ومن ثم، يوصى باستخدام عامل المسافة المعدل المقترح أو نموذج معدل المطر الفعال لتصميم قناة G5 في بيئة خارجية لنطاقات ترددات الموجات المليمترية قصيرة المدي ذات الموثوقية العالية. كما أظهرت الدراسة ان التوهين الناجم عن المطر يؤثر على حساب خسارة الانتشار، وأسّ خسارة المسير، وخبو الظل باستخدام نموذجين واسعي النطاق لخسارة مسار الخبو، وهما GPP3 وNYUSIM. يؤدي السلوك العشوائي للتوهين الناجم عن المطر إلى زيادة أس خسارة المسير (PLE = 2.79 عند $R_{0.01}$٪ 125 = مم / ساعة). قدم نموذج قناة NYUSIM تقديرًا أفضل للبيانات المقاسة لفقدان المسار مقارنةً بـ GPP3. تم تعديل نموذج خسارة مسار الإغلاق (CI) الذي تم تنفيذه بواسطة NYUSIM من خلال تضمين أس فقدان المسار وتلاشي الظل كدالة للنسبة المئوية للتوافر (٪ P من الوقت). نموذج خسارة المسير الاحتمالي المقترح، وهو مزيج من خسارة المسير في الفضاء الحر LOS المرجعي القريب، والتوهين الناجم عن المطر المستند إلى التوصية ITU-R P.530-17 المعدلة والتظليل عند الاحتمالات المختلفة، قادر على التنبؤ بخسارة المسير بشكل أكبر دقة في المناطق الاستوائية. كما اثبتت الدراسة لزيادة موثوقية الأداء في الوصلات الملمتريه بنسبة 99.99٪ خلال هطول الامطار فأن قيمة هامش تلاشي إضافي بمقدار 12 ديسيبل لازم لتعويض الفقد في الإشارات في المناطق الاستوائية. ستكون كل هذه النتائج مفيدة لتطوير نماذج قنوات G5 في بيئة خارجية، خاصة بالنسبة لموجة الملمتريه عبر مسارات قصيره المدي مع موثوقية عالية.

APPROVAL PAGE

This thesis of Asma Ali Hussein Budalal has been approved by the following:

_____
Md. Rafiqul Islam
Supervisor

_____
Khaizuran Abdullah
Co-Supervisor

_____
Tharek Abd. Rahman
Field Supervisor

_____
Teddy Surya Gunawan
Internal Examiner

_____
Mandeep Singh Jit Singh
External Examiner

_____
Mohamed Naqib Ehsan Jan
Chairman

DECLARATION

I hereby declare that this thesis is the result of my own investigations, except where otherwise stated. I also declare that it has not been previously or concurrently submitted as a whole for any other degrees at IIUM or other institutions.

Asma Ali Hussein Budalal

Signature ..... Date .....

INTERNATIONAL ISLAMIC UNIVERSITY MALAYSIA

DECLARATION OF COPYRIGHT AND AFFIRMATION OF FAIR USE OF UNPUBLISHED RESEARCH

MILLIMETER-WAVE PROPAGATION MODELING FOR 5G BASED ON RAIN FADE DATA IN TROPICAL CLIMATE

I declare that the copyright holders of this thesis are jointly owned by the student and IIUM.

No part of this unpublished research may be reproduced, stored in a retrieval system, or transmitted, in any form or by any means, electronic, mechanical, photocopying, recording or otherwise without prior written permission of the copyright holder except as provided below

1. Any material contained in or derived from this unpublished research may be used by others in their writing with due acknowledgement.

2. IIUM or its library will have the right to make and transmit copies (print or electronic) for institutional and academic purposes.

3. The IIUM library will have the right to make, store in a retrieved system and supply copies of this unpublished research if requested by other universities and research libraries.

By signing this form, I acknowledged that I have read and understand the IIUM Intellectual Property Right and Commercialization policy.

Affirmed by Asma Ali Hussein Budalal

……..…….. ……..

Signature Date

ACKNOWLEDGEMENTS

In the name of Allah, the most gracious and most merciful,

All praise is due to Allah (s w t); with Allah help, the thesis would have reached this stage. I would like to express my most sincere appreciation and gratitude to Professor. Md. Rafiqul Islam for his advice, guidance, suggestions, critical comments, and his tremendous supervision and continuous encouragement from the beginning. I will be forever grateful.

It is my utmost pleasure to dedicate this work to my parents. To my mother (Hameeda) for her endless support, love, and patience. To the spirit of my dear father (Ali Budalal), who taught us willpower and patience.

Finally, special acknowledgement to my dear husband (Abdel Karim), my daughters (Noha & Leena), and my sons (Aeemn & Idris) who granted me the gift of their unwavering belief in my ability to accomplish this goal despite my illness: thank you for their support and patience, I will be forever grateful to them.

TABLE OF CONTENTS

Abstract i
Abstract in Arabic ii
Approval Page iii
Declaration iv
Copyright Page v
Acknowledgements vi
Table of Contents vii
List of Tables x
List of Figures xii
List of Symbols xvi
List of Abbreviations ..... **Error! Bookmark not defined.**

CHAPTER ONE: INTRODUCTION 1
1.1 Overview and Motivation 1
1.2 Problem Statement 4
1.3 Research Objectives 6
1.4 Research Scope 7
1.5 Rechearch Philosophy 7
1.6 Rechearch Methodology 8
1.7 Thiesis Orgnization 10

CHAPTER TWO: LITERATURE REVIEW 12
2.1 Introduction 12
2.2 Millimetre Wave Propagation Characteristics 12
2.3 Challenges in Millimeter -wave Propagation 15
2.4 Outdoor Millimeter Wave Propagation Channels 20
2.4.1Channel large–scale parameters (LSPs) definition 21
2.4.2 Path Loss in Urban Microcell Environments 21
2.4.3 The Propagation Parameters Effect Path Loss Modelling 23
2.4.4 Path loss model 24
2.5 NYUSIM Channel Model 26
2.6 3GPP Channel Model 30
2.7 Loss Studies in Tropical Climate 32
2.8 Rain-Induced Fading in mm-wave 34
2.8.1 Rain Fade Impact on short-range fixed Millimeter Wave links 39
2.8.2 Rain Attenuation prediction models 44
2.8.3 Inaccuracy Estimation of Rain Fade Over a Short Path 51
2.9 Summary 54

CHAPTER THEE: RESEARCH METHODOLOGY 56
3.1 Introduction 56
3.2 Research Process And Flow Chart 57

3.3 Measurements Of Rain Rate And Rain Attenuation 62
3.4 Measurements Of Rain Attenuation 63
3.4.1 Conversion from AGC to Receive Signal Level..... 65
3.4.2 Rain Attenuation Data 68
3.5 Large-Scale Path Loss Model..... 71
3.5.1 Simulation of Path Loss in 3GPP TR 38.900 Channel Model 75
3.5.2 Simulation of Large-Scale Path Loss Model in NYUSIM 76
3.6 Summary..... 78

CHAPTER FOUR: MODIFICATION AND VALIDATION OF ITU-R P.530-17 MODEL 80
4.1 Introduction 80
4.2 Rain Rate And Rain Attenuation Distribution..... 80
4.2.1 Statistical Analysis of Rain Rate 80
4.2.2 Statistical Analysis of Rain Attenuation..... 82
4.3 Measurement Versus Prediction Models..... 85
4.3.1 Measurement Vs. Prediction At 26 GHz and 38 GHz 87
4.3.2 Other Measurement..... 87
4.3.3 Observations from Measurements 88
4.4 Frequency Scaling Analysis 89
4.5 Distance Factor Investigation 91
4.6 Proposed Modification Of Distance Factor 95
4.7 Modelling Of Increment Factor..... 97
4.8 Validation Of Modified Model..... 100
4.8.1 Validation Using 26 Ghz And 38 Ghz Measurement 101
4.8.2 Validation Using Other Measurement..... 101
4.9 Concept Of Effective Rain Rate R_eff 105
4.10 Modelling Of Effective Rain Rate Concept 107
4.11 Validation Of Effective Rain Rate Concept 107
4.12 Estimation Of Error In Prediction 113
4.13 Summary..... 114

CHAPTER FIVE: EFFECT OF RAIN ATTENUATION ON PATH LOSS .. 117
5.1 Introduction 117
5.2 Propagation Characteristics Analysis Considering Rain 118
5.2.1 Free Space Loss 118
5.2.2 Directional path loss calculation from Measured PRX [dBm] 119
5.2.3 Path Loss Estimation at Different Distances 122
5.2.4 Pathloss Exponent..... 124
5.2.4.1 Estimation of Pathloss Exponent During Clear Sky 125
5.2.4.2 Estimation of Pathloss Exponent During Rain Events 125
5.2.5 Estimation of Shadow Fading (SF) 127
5.3 Diurnal Effect On Path Loss Observed In Malaysia 128
5.4 Comparison Between Estimated Path Loss From Measured Data With Those Predicted By Models..... 130
5.5 Modification Of CI Model..... 133
5.6 Proposed Probabilistic CI Model..... 137
5.7 Probability of PL Greater Than Threshold (γ) because of Shadowing... 141

5.8 Summary.....145

CHAPTER SIX: CONCLUSION FUTURE WORK 147
6.1 Introduction 147
6.2 Contributions 151
6.3 Recommendation And Future Work.....152

REFERENCES.....153
APPENDIX A: LIST OF PUBLICATIONS.....170
APPENDIX B 171
APPENDIX C 173
APPENDIX D 174

LIST OF TABLES

Table 2.1	Comparison of Some Recent Publications Related Work in Outdoor Urban Millimetre Wave Propagation	33
Table 2.2	Summary of rain attenuation measurements implemented at mm-wave frequencies in different climate regions in over the world (d≥1km)	47
Table 2.3	Summary of rain attenuation measurements implemented at millimeter-wave Short-Range Fixed Links in different climate regions in over the world (d≤1km)	48
Table 3.1	Summary of links parameters for the 26 GHz and 36 GHz	62
Table 3.2	Sample of Raw Data Received Signal Level at 38Ghz	70
Table 3.3	Pathloss models	76
Table 3.4	The Detailed Configuration for NYUSIM Simulations	77
Table 4.1	Annual rain rate distribution Rain rate exceedance	81
Table 4.2	Comparison of rain attenuation measured at frequencies < 40 GHz in different climate regions and those predicted using the proposed model	103
Table 4.3	Comparison of rain attenuation prediction using the proposed effective rain rate concept and those measured at frequencies > 40 GHz as the data is extracted from the 300-m 73.5 and 83.5 GHz LOS terrestrial link	104
Table 4.4	The increment factor of specific attenuation proposed from measured data at (26GHz,38GHz, 73GHz and 83GHz over 300m) at different rain rates in mm/h.	111
Table 4.5	Comparison of rain attenuation prediction using the proposed effective rain rate concept and those measured at frequencies > 40 GHz as the data is extracted from the 300-m 73.5 and 83.5 GHz LOS terrestrial link	112
Table 5.1	Path loss (PL_m) Derived from Measured ($PRX\ [dBm]$) at 38GHz link	120
Table 5.2	Range of PLE values in different scenarios	124

Table 5.3	The estimated value of PLE extracted from measured PRX [dBm]) with considering rain attenuation	126
Table 5.4	The PLE values in extreme rainy weather for LOS outdoor measurements at 38 GHz in Malaysia	129
Table 5.5	Adjusted R-squared)	135
Table 5.6	Comparison of the PL according to NYUSIM model: In UMi and LOS scenario for the parameters of at 38GHz (temperate areas and tropical)	136

LIST OF FIGURES

Figure 1.1	Millimetre-wave spectrum with expected bandwidth	2
Figure 2.1	Mm-wave propagation characteristics.	14
Figure 2.2	A typical wireless communication channel	15
Figure 2.3	Demonstrates major parameters, used for mm-wave channel measurements	16
Figure 2.4	Atmospheric absorption across electromagnetic waves in dB/km	18
Figure 2.5	Rain attenuation across frequency at various rainfall intensities	19
Figure 2.6	Impact of rainfall in the propagation of mm-wave channel	38
Figure 2.7	Propagation attenuation due rain at mm-wave frequencies with various rain rate, frequency bands, and different path length	38
Figure 2.8	Impact of effective length on the rain fade with rain intensity of 30 mm/hr based on ITU (ITU-R) 530-14 Model	39
Figure 2.9	Comparison of the predicted rain attenuation values exceeded for 0.01% of the time ($A_{0.01}$) against transmitter-receiver path distance at 28GHz.	41
Figure 2.10	Comparison of the CCDF of estimated rain attenuation values at 28 and 38 GHz	39
Figure 2.11	SNR as a function of distance and weather conditions	40
Figure 2.12	The Attenuation different frequencies over short path length measured in Singapore.	41
Figure 3.1	Research flow chart	61
Figure 3.2	Rain Rate Data Logging Systems (Casella).	62
Figure 3.3	The top view of the Location of the path link from Google Earth	64

Figure 3.4	The block diagram of the experimental setup	65
Figure 3.5	RF input level as a function of AGC level.	66
Figure 3.6	RF input level as a function of AGC level for MINI-LINK 38E.	67
Figure 3.7	Measured rain rate and rain attenuation on experimental Mini-links at 26 and 38 GHz during raining event from	70
Figure 3.8	Pathloss phenomenon in clear air 38 GHz	72
Figure 3.9	Pathloss phenomenon in rainy air at 38 GHz over 300m path length	73
Figure 3.10	Research flow chart to estimate Path loss from the measured data	74
Figure 3.11	Definition of d_{2D} and d_{3D} for outdoor UTs in the 3GPP model	75
Figure 3.12	A graphical user interface (GUI) for NYU's channel simulator	78
Figure 4.1	One-year measurement in Malaysia is presented as rain rate's cumulative distribution	82
Figure 4.2	Probability distributions of measured one-year rain attenuation at 26GHz and 38GHz over the path length of 300 m.	83
Figure 4.3	Measured rain rate vs. rain attenuation at 26GHz and 38GHz	84
Figure 4.4	Total number of fade events for a given fade amplitude measured at 38 GHz microwave link with 300 m path length.	84
Figure 4.5	Probability of occurrences of rain attenuation for different measured attenuation levels at 38 GHz at 300 m path length.	85
Figure 4.6	CCDF of measured rain attenuation at 26GHz and 38GHz and those predicted by models.	86

Figure 4.7	Comparison between CCDF of measured rain attenuation at 75GHz (Shrestha and Choi,2017) and 25GHz (Hasan et al.,2012) and those predicted by ITU-R P.530 17.	87
Figure 4.8	Comparison between measured rain attenuation at 38GHz and that predicted by frequency scaling from attenuation statistics at 26GHz	90
Figure 4.9	Comparison between measured rain attenuation at 26 GHz and that predicted by frequency scaling from attenuation statistics at 38 GHz	90
Figure 4.10	Variations of path reduction factor values with distance in ITU-R P.530-17.	94
Figure 4.11	α Coefficient at vertical polarization	95
Figure 4.12	Comparison of measured rain attenuation CCDF with those predicted by the proposed modified model in Malaysia for 300 m path length.	101
Figure 4.13	Comparison of measured rain attenuation CCDF with those predicted by the proposed modified model at 25 GHz with 223 m in Japan and 75 GHz with 100 m in Korea	102
Figure 4.14	Effective rain rate against 1-min rain rate at different distances <1km.	106
Figure 4.15	Comparison of measured and predicted rain attenuation in Malaysia using R_eff technique at 73GHz over 300m. R_(%p),>100 (mm/h)	109
Figure 4.16	Comparison of measured and predicted rain attenuation in Malaysia using R_{eff} technique at 83GHz over 300m. $R_{\%p} > 100$ (mm/h).	110
Figure 4.17	Rain attenuation prediction at 38GHz and path length <1km.	112

Figure 5.1	Comparison of path loss in dB, between rainy days and no rain event, at Malaysia versus the logarithm of distance in m at a frequency of 38 GHz	123
Figure 5.2	Diurnal variation of path loss measured at 38 GHz for 300 m path	128
Figure 5.3	Comparison of free-space, CI, and 3GPP path loss models with path loss estimated from measured data at 38 GHz for the UMi LOS environment	131
Figure 5.4	Comparison between the path loss predicted by Close-In, modified CI and 3GPP models with that estimated from measured data.	134
Figure 5.5	Comparison between proposed probabilistic path loss model in temperate region with PL analytically estimated from measured data over 300m at 38GHz.	139
Figure 5.6	Estimated value of path loss over different Tx-Rx separation (m) with considering rain attenuation at different (%) of the time for the proposed model with LOS for the outdoor terrestrial link in 28 ◦C rain (htx = hrx = 18 m) ($\chi\sigma$ = 5.22dB	140
Figure 5.7	Path loss in dB vs distance in meters at different probability level at 38GHz	140
Figure 5.8	Probability of directional PL greater than a certain threshold for a small percentage of time or location in the cell	142
Figure 5.9	Link margin at different reliability level for 38GHz over 300m	144

LIST OF ABBREVIATIONS

ITU-R	International Telecommunication Union- Radio Sector
DSD	Drop Size Distribution
CD	Cumulative Distribution
PDF	Probability density function
CDF	Cumulative Distribution Function
BER	Bit Error Rate
SNR	Signal to Noise Ratio
FM	Fade Margin
BW	Band Width
FSPL	Free Space Path Loss
EiRP	Effective Radiated Power
3GPP	3rd Generation Partnership Project
5G	Fifth Generation
BER	Bit Error Rate
CIR	Channel Impulse Response
FSL	Free-Space Loss
MIMO	Multiple-Input Multiple-Output
NLOS	Non-Line-of-Sight
OFDM	Orthogonal Frequency Division
SINR	Signal to Interference Plus Noise Ratio
DS	Delay Spread
O2I	Outdoor-to-indoor

SUI	Stanford University Interim
ABG	Alpha-Beta-Gamma (ABG)
ULA	Uniform Linear Array
URA	Uniform Rectangular Array
HPBW	Half Power Beamwidth
UMi	Urban Microcell
UMa	Urban Macrocell
RMa	Rural Macrocell
Co-Pol	Co-polarized
X-Pol	Cross-polarized
PLE	Path Loss Exponent
RMS	Root-Mean-Square
ISI	Inter Sample Interference
KF	Rician K-factor (KF)
FM	Fade Margin FM
CDF	Cumulative Distribution Function
AT	Attenuation Factor
PDP	Power Delay Profile
CW	Continuous Wave
SF	Shadow Fading SF
SSCM	Statistical Spatial Channel Model
O2I	Outdoor-to-indoor
URC	Ultra-Reliable Communication
PER	Packet Error Rat

LIST OF SYMBOLS

A	Attenuation level in dB
$A_{0.01}$	Attenuation exceeds for 0.01% of the time in dB
d	Path length
D	Drop diameter
D_0	Drop mean diameter
La	Atmospheric losses
d_0	Reference distance d_0
n	Path loss exponent
γR	Specific Attenuation of rain in dB/km
E	Expected value
f	Frequency in Hz
R_{eef}	Effective rain rate in mm/hr
NF	Noise figure
W	Channel simulation bandwidth
α	Attenuations factor dB/m
L_0	Path loss at the reference distance d0
Agas	Atmospheric gases
Q	Q function
A_{rain}	Attenuated by rain
χσ CI $_1$	Shadow factor in dB
$PL(d_0)$	Path loss at the reference distance d_0
β	The thunderstorm ratio

k and α	Frequency and polarization dependent coefficients
$N(D)$	Drop size distribution
r	Path reduction factor
P_r	Received power
P_t	Transmitted power
R	Rain rate in mm/hr
$R_{0.01\%}$	Rain rate exceeded for 0.01% of the time in mm/hr
$R_{0.001\%}$	Rain rate exceeded for 0.001% of the time in mm/hr
$d_0(R_p)$	Equivalent cell diameter
RSL_{clear}	RSL during clear sky
RSL	RSL during rain
PRX	Received power,
GTX	Transmit antennas' gains
GRX	Receiver antennas' gains
$PL\ [dB]$	Path loss
$\overline{PL}$	Mean value of the measured path loss at 300 m
d_i	Distance between the Tx and the Rx
σ	Standard deviation about the mean
ψ	The standard deviation of shadow fading
$prob(\%)$	Percentage of time
ψ	The standard deviation of shadow fading
(γ)	Threshold value of path loss
ρ	Reliability

CHAPTER ONE

INTRODUCTION

1.1 GENERAL BACKGROUND AND MOTIVATION

The current microwave band, typically below 6 GHz, has been fully utilised and progressively congested. For this reason, mm-wave technology captures the research community's high interest as these potential channels for supporting extremely high data rate in future wireless systems (Rappaport et al., 2013; Karagiannidis et al., 2017; Petrov, 2020). Furthermore, the mm-Waves band has substantial access to 10 Gbit/s bandwidth with the maximum data rates (Sun et al., 2018). In light of this, mm-wave is strongly recommended for future services and applications such as real-time video streaming and the rise of the Internet-of-Things (Rappaport et al., 2017).

Mm-wave and small cells can be coordinated to data transmission links and backhaul by utilizing the same frequency band (Liu et al.,2019). However, mm-wave considered the extremely high frequency (theoretically range from 30 GHz–300 GHz) with wavelengths ranging from 1 to 100 mm (Lam et al.,2017). Because of the small wave length of mm-waves It is possible to pack many high-gain antennas array on-chip into the mm-wave transceivers due to the very small wavelength at mm-wave frequencies. Additionally, CMOS technology can utilize well into the mm-wave frequency bands cost-effectively (Gupta & Jha.,2015). Mm-wave technology in mobile systems can employ highly directional antenna radiation patterns using beamforming to gain better spectral efficiency,

overcome propagation losses, and decrease interference's influence. Mm-wave is characterized by inherent security and privacy because of narrow beamwidth.

Furthermore, mm-wave technology is also qualified as power- and noise-limited rather than bandwidth- and interference-restricted for conventional mobile systems (Jasim, 2018). One significant benefit of the mm-wave spectrum is that it offers long, continuous band allocations at significantly reduced licensing costs, which is much lower than the microwave band (Hong, 2018). Therefore, it can be utilized to provide high throughput in a small geographic area. The latest ITU World Radiocommunication Conference 2019 (WRC-19) WRC-19 proposed by the ITU states that 24-86 GHz bands will be considered for 5G. The simplified frequency spectrum and bandwidth chart presented by the ITU is represented in Figure 1.1. Many countries have started arranging commercial 5G networks focusing on the spectrum range 26.5 GHz to 29.5 GHz (Han et al.,2019).

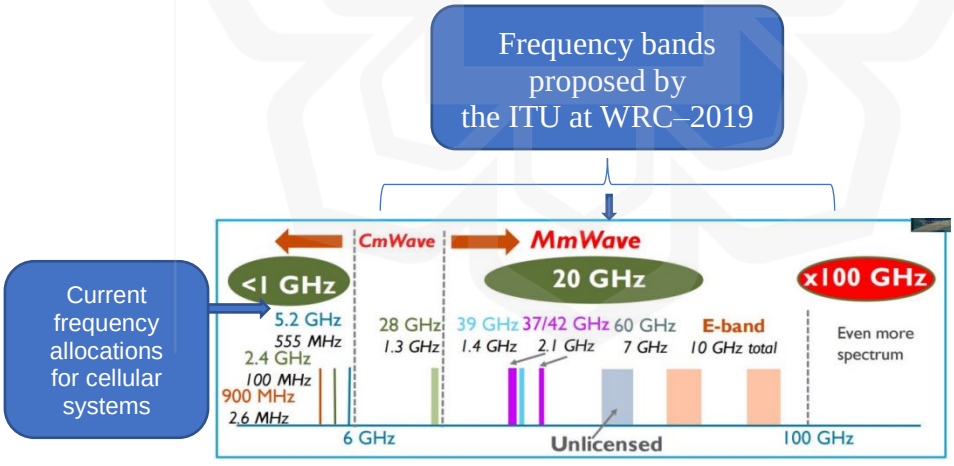

Figure 1.1 Millimeter-wave spectrum with expected bandwidth source: (Shimodaira et al., 2015)

However, few challenges faced by wideband communications for terrestrial mobile applications become clear and must be solved (Rappaport et al.,2013; Wei et al.,2014;

Rangan et al.,2014; Xiao et al.,2018). Like other cellular communication systems, the applications of mm-wave frequency-based 5G mobile networks in a specific environment require comprehensive knowledge of the propagation features.

Mm-wave frequencies suffer from severe propagation losses compare to the sub-6 GHz frequency band. The propagation parameters, such as path loss, frequency-dependence material penetration loss, propagation mechanism (i.e., reflection diffraction, scattering), delay spread, atmospheric attenuation oxygen absorption, and the effect of rain, foliage, and other attenuation losses are adopted to characterize the radio propagation channels (Hemadeh et al., 2018; Rappaport et al., 2017). These parameters can be acquired mainly by reviewing the measurement of data campaigns conducted in diverse environments. Because of these propagation impairments, mm-wave signals' utilisation has been confined to particular applications such as indoor services or short-range communications. Ultimately, the development and implementation of accurate propagation models are vital for wireless communication, starting from equipment design, system design, optimization, and performance. Hence, channel modelling is a significant supplier to link and system-level performance (Ju et al., 2019; Han et al., 2020).

Most notably, since each country has diverse climate factors and terrain profile, it necessitates a channel model of 5G developed autonomously to realize a particular area's best performances. Until now, the stud of mm-wave propagation for 5G applications in the outdoor environment is still limited. In light of this, many researchers worldwide have become increasingly interested in this regard, but tropical regions remain insufficiently investigated.

In the design of 5G systems and beyond, fading characteristics due to high rainfall and atmospheric propagation are considered the most significant challenges to improving system capacity and meeting quality and ultra-reliability criteria (Zhang et al.,2019; Han et al.,2020). A formulation of the rain fade and directional path loss for short-range transmission requires extensive propagation measurement at various path length data at different climatic zones for complete modelling of rain attenuation phenomenon (Shayea et al., 2018; Huang et al., 2019; Shrestha and Choi., 2019; Luini et al., 2019; Akron., 2019). Therefore, the study of tropical outdoor mm-wave channel description is significantly related to preparing mm-wave-based 5G applications with short ranges. To implement, establish, and maintain good-quality mm-wave links for directional transmission in a small cell in the tropical climate, rain characteristics and its impact on mm-wave propagation must be embedded in channel modeling based on tropical measurements. This research has investigated and modeled mm-wave propagation for outdoor mm-wave channels in the tropical environment based on rain intensity and rain attenuation data at mm-wave propagation measured in the Malaysian tropical climate.

1.2 PROBLEM STATEMENT AND ITS SIGNIFICANCE

5G technology is proposed as a great opportunity based on the mm-wave frequency band. Hence more research to investigate the possibilities and challenges of developing these valuable resources is an urgent requirement. Utilizing mm-wave in outdoor environments is still a considerable challenge. Intrinsically high path loss with distance from the transmitter to the receiver is causing large signal strength variability between LoS and NLoS conditions which causes a challenge to establish coherent communication.